

# Fracture analysis of quadruple fastenings with bonded anchors

Y.-J.Li, R.Eligehausen, B.Lehr & J.Ozbolt

*Institute for Construction Materials, Stuttgart University, Germany*

**ABSTRACT:** In order to investigate the failure mechanism and the failure load of quadruple fastenings with bonded anchors a series of numerical investigation was carried out. The studied specimens were bonded anchors in a concrete block and subjected to tensile loading. In the calculations the microplane model with relaxed kinematic constraint was used to simulate the concrete and bond materials. Totally more than 50 calculations were performed. Varied were embedment depth ( $h_{ef} = 4d$  to  $20d$ ), spacings between anchors ( $s = 0.25h_{ef}$  to  $2.5h_{ef}$ ), anchor diameter ( $d = 8, 12$  and  $20$  mm) and bond strength ( $\tau_b = 6.2$  to  $22.5$  N/mm<sup>2</sup>). The results of the numerical studies were compared with the results of experimental investigations. From these studies the failure mechanism of bonded group anchors is clearly revealed and the group effect on the failure load is clarified. Based on the numerical and experimental results a model for evaluating the failure load of quadruple fastenings with bonded anchors is proposed.

## 1 INSTRUCTION

A bonded anchor consists of a reinforcing bar or a threaded rod inserted into a hole drilled in hardened concrete which is filled with a bonding agent. During the last 2 decades several research works on bonded anchors have been published (Eligehausen, Mallee & Rehm, 1984, 1997; Eligehausen, Lehr, Meszaros & Fuchs, 1999; Cook, Doerr & Klingner, 1993; Cook, Kunz, Fuchs & Konz, 1998). The failure process and the failure mechanism of single bonded anchors have been investigated and design recommendations have been proposed both for single anchors (Eligehausen, Mallee & Rehm, 1984; Eligehausen, Lehr, Meszaros & Fuchs, 1999; Cook, Kunz, Fuchs & Konz, 1998) and for group anchors (Eligehausen, Mallee & Rehm, 1984; Eligehausen, Lehr, Meszaros & Fuchs, 1999). However the design recommendation for group anchors are valid only for bonded anchors with an embedment depth  $h_{ef} \sim 9d$ . For bonded group anchors with a spacing smaller than a critical value it is found that the failure load is reduced with decreasing spacing (Lehr & Eligehausen, 1998). This phenomenon is called group effect. Evidently the group effect and the failure mechanism of group anchors should be strongly influenced by spacing between anchors, embedment depth, anchor diameter and bond strength. The main purpose of this work is to study numerically the failure mechanism and the group effect of quadruple fastenings with bonded anchors by varying the spacing between anchors, the embedment depth, the anchor diameter and the bond strength.

The studied specimens are bonded anchors of the injection type based on resin mortar anchored into a concrete block and subjected to tensile loading. The considered anchor group is quadruple. A series of experiments have been performed during the last years (Lehr & Eligehausen, 1998). From the experiments it is known that with variation of embedment depth and/or spacing among anchors the failure mode varies from concrete cone failure to pullout failure. When the spacing is not large enough the failure load is smaller than 4 times the failure load of a single anchor even when pullout failure occurs. In order to investigate the failure mechanism in more detail and to understand the experimental results, a numerical parameter study has been carried out with variation of the embedment depth ( $h_{ef} = 4d$  to  $20d$ ), the spacing between anchors ( $s = 0.25h_{ef}$  to  $2.5h_{ef}$ ), the anchor diameter ( $d = 8, 12$  and  $20$  mm) and the bond strength ( $\tau_b = 6.2$  to  $22.5$  N/mm<sup>2</sup>). The calculation was performed with the 3D nonlinear finite element program MASA, in which the newly developed microplane model with relaxed kinematic constraint (Ozbolt, Li & Kozar, 2000) is implemented. Based on the numerical and experimental results a model for evaluating the failure load of quadruple fastenings with bonded anchors is proposed.

## 2 NUMERICAL ANALYSIS OF QUADRUPLE ANCHOR GROUPS

The analyzed specimen is shown schematically in Figure 1. A typical finite element mesh with load

and boundary conditions is shown in Figure 2. Due to symmetry, only a quarter of the specimen is simulated. The simulated system includes the steel anchors, the adhesive mortar and the concrete block. The steel anchor is assumed as a linear elastic material with Young's modulus  $E = 210000 \text{ N/mm}^2$  and Poisson's ratio  $\nu = 0.3$ . The concrete is modeled by the newly developed microplane model (Ozbolt, Li & Kozar, 2000) and the material parameters are taken as Young's modulus  $E = 30000 \text{ N/mm}^2$ , Poisson's ratio  $\nu = 0.18$ , tension strength  $f_t = 2.4 \text{ N/mm}^2$ , compression strength  $f_c = 30 \text{ N/mm}^2$  and fracture energy  $G_f = 0.1 \text{ N/mm}$ . The compressive fracture energy is taken as 200 times the tensile fracture energy.

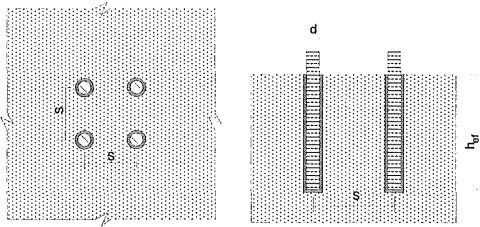


Fig. 1 Geometry of quadruple fastening with bonded anchors

In most calculations the bond material is simulated by a special interface model with an average shear strength  $\tau_i \sim 12 \text{ N/mm}^2$ . This interface model is based on the normal microplane model but only the shear resistance is considered (Ozbolt, 1998). The numerical study shows that with this model the influence of lateral stresses on the shear behavior as found in the tests by Meszaros and Eligehausen (1998) could be simulated. To study the influence of different bond strength values on the group effect the bond material is simulated by the microplane model with three

different bond strengths as  $\tau_i = 6.2 \text{ N/mm}^2$ ,  $\tau_i = 11.1 \text{ N/mm}^2$  and  $\tau_i = 22.5 \text{ N/mm}^2$ , respectively. The bond strength is calibrated by the calculation of a confined single anchor pull-out test with an embedment depth  $h_a = 100 \text{ mm}$ , which corresponds to the dimension of the specimen used by Meszaros and Eligehausen (1998). The load is applied at the top end of the steel anchor. Displacement control is used in order to get the post peak load-displacement curve. A fixed boundary condition, corresponding to the support lines in experiments, is applied on the non-symmetry edges at the loaded side of the specimen.

In order to confirm the simulation capability of the newly developed microplane model and the interface model two typical experiments of quadruple bonded group anchors, performed by Lehr and Eligehausen (1998) with different failure modes were simulated, one is a concrete cone failure and another one is a pullout failure. The numerical results show that the calculated load-displacement curves and failure modes agree well with the experimental data. The difference in maximum loads between the values obtained from tests and simulations are less than 10% (Li, Ozbolt, Eligehausen & Lehr, 1999).

The systematical study of the failure mechanism and the group effect on the failure load was performed with anchor diameter  $d = 12 \text{ mm}$ . Totally 26

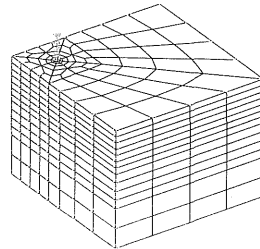


Fig. 2 Finite element mesh

Table 1. Numerical and experimental results with  $d = 12 \text{ mm}^1$

| $h_d$<br>[mm] |    | Single |            | Spacing $s$ [mm] |            |       |            |       |            |       |            |       |            |       |            |
|---------------|----|--------|------------|------------------|------------|-------|------------|-------|------------|-------|------------|-------|------------|-------|------------|
|               |    |        |            | 48               |            | 96    |            | 144   |            | 192   |            | 216   |            | 240   |            |
|               |    | $F_u$  | $F_M^{2)}$ | $F_u$            | $F_M^{2)}$ | $F_u$ | $F_M^{2)}$ | $F_u$ | $F_M^{2)}$ | $F_u$ | $F_M^{2)}$ | $F_u$ | $F_M^{2)}$ | $F_u$ | $F_M^{2)}$ |
| 48            | Ca | 20.4   | CC         | 50.1             | CC         | 66.0  | CC         | 76.7  | CC         | 76.1  | CCB        |       |            |       |            |
|               | Ex | 16.1   | CC         | 38.2             | CC         | 52.0  | CC         | 66.6  | CCB        |       |            |       |            |       |            |
| 96            | Ca | 40.2   | PO         | 98.4             | CC         | 124   | CC         | 142   | CC         | 145   | PO         |       |            | 149   | PO         |
|               | Ex | 38.6   | CCB        | 81.4             | CC         | 96.2  | CC         | 129   | CC         | 149   | CCB        |       |            | 183   | CCB        |
| 144           | Ca | 54.4   | PO         | 132              | CCB        | 180   | CCB        | 211   | FPO        |       |            | 221   | PO         |       |            |
|               | Ex | 61.7   | PO         | 106              | CCB        |       |            | 192   | PO         |       |            | 212   | PO         |       |            |
| 192           | Ca | 77.2   | PO         | 196              | CCB        | 246   | FPO        | 278   | FPO        | 284   | PO         |       |            |       |            |
|               | Ex | 72.4   | PO         |                  |            |       |            |       |            | 258   | PO         |       |            |       |            |
| 240           | Ca | 92.7   | PO         | 251              | CCB        | 312   | FPO        | 341   | PO         |       |            |       |            | 356   | PO         |
|               | Ex |        |            |                  |            |       |            |       |            |       |            |       |            |       |            |

1):  $F_u$ : Failure load [kN];  $F_M$ : Failure mode; Ca: Calculations; Ex: Experiments

2): CC, CCB, PO, FPO: different failure modes, see section 3.1

cases were calculated with the variation of embedment depth  $h_{ef} = 48 \text{ mm}$  to  $h_{ef} = 240 \text{ mm}$  ( $h_{ef} = 4d$  to  $h_{ef} = 20d$ ) and the spacing between anchors from  $s = 48 \text{ mm}$  to  $s = 240 \text{ mm}$  ( $s = 0.2h_{ef}$  to  $s = 2.5h_{ef}$ ). The analyzed specimens with calculated failure loads and failure modes are listed in Table 1 and if available the corresponding average failure loads and the failure modes observed in the experiments by Lehr and Elgehausen (1998) are indicated as well. Additionally the experimental and numerical results of single anchors with different embedment depths are listed together with the correspondent group.

The influence of the anchor diameter on the group effect was investigated with additional 9 calculations, which include 4 cases with  $d = 8 \text{ mm}$  and 5 cases with  $d = 20 \text{ mm}$ . In the calculations the material properties both for concrete and for bond mortar remained the same as the calculations in Table 1. The embedment depth was kept constant as  $h_{ef} = 144 \text{ mm}$  and the spacing were varied from  $s = 48 \text{ mm}$  to  $s = 240 \text{ mm}$ . The calculation results are listed in Table 2.

Table 2. Numerical results with  $d = 8 \text{ mm}$  and  $d = 20 \text{ mm}$ <sup>1)</sup>

| Spacing<br>$s$<br>[mm] | $d$ [mm]   |       |            |       |
|------------------------|------------|-------|------------|-------|
|                        | 8          |       | 20         |       |
|                        | $F_u$ [kN] | $F_M$ | $F_u$ [kN] | $F_M$ |
| 0                      | 45.3       | PO    | 76.7       | PO    |
| 48                     | 130        | CC    |            |       |
| 96                     | 160        | FPO   | 203        | CC    |
| 144                    | 165        | PO    | 241        | FPO   |
| 180                    |            |       | 257        | PO    |
| 240                    |            |       | 273        | PO    |

1):  $F_u$ : Failure load;  $F_M$ : Failure mode

In order to investigate the influence of bond strength on the group effect another 21 calculations were performed, which include 18 cases for group anchors and 3 cases for single anchor. Three different bond strength values were considered, namely a high bond strength with  $\tau_n = 22.5 \text{ N/mm}^2$ , an average bond strength with  $\tau_n = 11.1 \text{ N/mm}^2$  and a low bond strength with  $\tau_n = 6.2 \text{ N/mm}^2$ . In the calculations the spacing between anchors was varied from 48 mm to 288 mm but the anchor diameter  $d$  and the embedment depth  $h_{ef}$  remain constant as  $d = 16 \text{ mm}$  and  $h_{ef} = 96 \text{ mm}$ . In a preliminary study a shear failure in the concrete near the bond layer was observed in the cases with a high bond strength. In order to avoid this shear failure the width of the elements used for the bond layer is extended from 2 mm to 6 mm. The dimension of the elements near the bond layer remained constant for all calculations. The load-displacement curves at the loaded side of the anchor were calculated and the failure modes are investi-

gated. The calculated failure loads and failure modes are presented in Table 3.

Table 3 Numerical results with different bond strength values<sup>1)</sup>

| $s$<br>[mm] | Bond strength $\tau_n$ [N/mm <sup>2</sup> ] |       |       |       |       |       |
|-------------|---|-------|-------|-------|-------|-------|
|             | 6.2   |       | 11.1  |       | 22.5  |       |
|             | $F_u$                                       | $F_M$ | $F_u$ | $F_M$ | $F_u$ | $F_M$ |
| 0           | 29.96                                       | PO    | 53.78 | PO    | 65.72 | CC    |
| 48          | 20.95                                       | CCB   | 25.18 | CC    | 23.79 | CC    |
| 96          | 24.74                                       | FPO   | 31.34 | CC    | 31.47 | CC    |
| 144         | 28.46                                       | PO    | 40.30 | FPO   | 42.41 | CC    |
| 192         | 28.94                                       | PO    | 46.68 | PO    | 51.95 | CC    |
| 240         | 29.19                                       | PO    | 48.01 | PO    | 58.24 | CC    |
| 288         | 30.05                                       | PO    | 50.31 | PO    | 59.05 | CC    |

1):  $F_u$ : Failure load [kN];  $F_M$ : Failure mode

In all calculations the material parameters of concrete are kept constant as given before. The dimension of the simulated concrete block is 400 mm times 400 mm wide with a depth of  $h_{ef} + 188 \text{ mm}$ , which has been shown enough to simulate a non-confined pull-out structure (Li, Ozbolt, Elgehausen & Lehr, 1999).

### 3 NUMERICAL RESULTS

#### 3.1 Failure modes

In the calculations four types of failure mode were observed which are schematically shown in Figure 3 and listed in Table 1 to Table 3 as: concrete cone (CC) failure, bond (pullout; PO) failure, combined concrete cone and bond (CCB) failure and false pullout (FPO) failure.

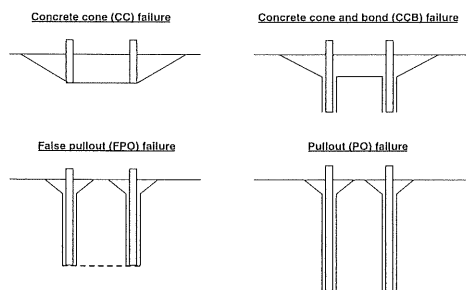


Fig. 3 Failure modes observed in the numerical analysis

In experiments the first three failure modes can easily be identified from the final failure form of the pullout test but the last one, so-called false pullout failure, can not be seen directly. This failure mode was observed in some calculations. It is characterized by cracks which initiated at the end of the anchors, propagated towards each other and connected

at peak load at the end of the anchors (see Figure 4 b). This crack can also be seen in the deformed mesh (see Figure 4 a). Because the concrete around the outside of the anchor group is strong enough to resist the applied load the final rupture occurred in the bond layer i.e. the final failure mode is a pullout failure. Although this failure mode at concrete surface looks like a pullout failure the loading capacity is reduced compared to a real pullout failure. Therefore we call this type of failure as “false pullout failure”.

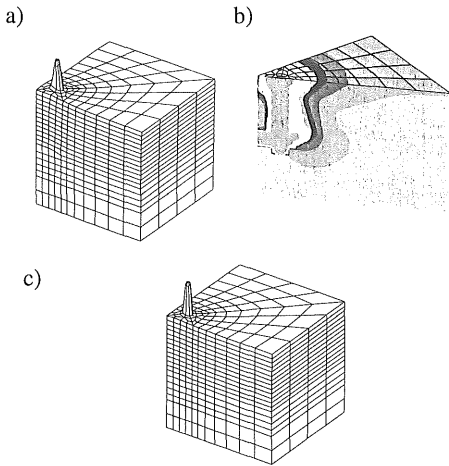


Fig. 4 False pullout failure a) deformed mesh at peak load; b) failure mode on diagonal section at peak load (maximum principal strain); c) final deformed mesh at post peak

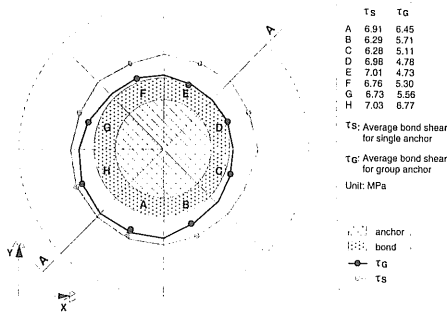


Fig. 5 Distribution of shear stresses around anchor perimeter

In order to understand the reason of the reduced failure load in the case of false pullout failure the shear stress distribution at peak load around the perimeter and along the embedment depth of group anchor is investigated and compared with the shear stress distribution valid for a single anchor. The results are shown in Figures 5 and 6, which are valid

for  $d = 12 \text{ mm}$ ,  $h_{ef} = 192 \text{ mm}$  and  $s = 96 \text{ mm}$ . The calculated failure load of the group is  $F_u = 246 \text{ kN}$ , which is about 25% lower than 4 times the calculated failure load of a single anchor (compare Table 1). Figure 5 shows that the distribution of shear stresses is almost axisymmetric for a single anchor while for the group anchors the shear stresses at the part of perimeter outwards the neighboring anchors are evidently smaller than those at opposite side.

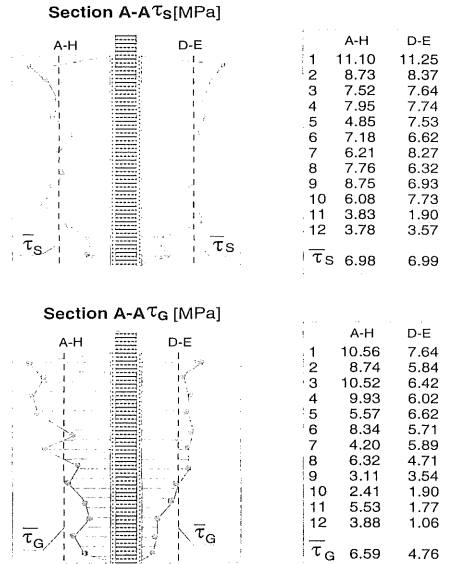


Fig. 6 Distribution of shear stresses along anchors

In Figure 6 the shear distribution along the embedment depth is shown for the sections A-H and D-E, which represent the positions of the section located towards and outwards neighboring anchors respectively.  $\tau_s$  and  $\tau_g$  are the shear stresses at peak load of single and group anchors. It can be seen that the shear stress distribution and the average shear stresses of a single anchor are almost identical at both sides of the anchor rod as  $\tau_u = 6.98 \text{ N/mm}^2$  and  $\tau_u = 6.99 \text{ N/mm}^2$ , respectively. But for the group anchor the shear stress distributions at both sides of the anchors are significantly different. The average shear stress amounts to  $6.59 \text{ N/mm}^2$  in section A-H and  $4.76 \text{ N/mm}^2$  in section D-E. Therefore the average shear stress towards the neighboring anchors is not much reduced compared to the value for single anchors, while the average shear stress at the opposite side (outwards the neighboring anchors) is about 30% smaller. Further study indicates that the reduction of the shear resistance at the side outwards the neighboring anchors is mainly caused by an increase of lateral tensile stresses in concrete because of the damage at the bottom of anchors. As shown in the

experiments by Meszaros & Eligehausen (1998) lateral tensile stress can significantly reduce the shear resistance of the bond material. This is the main reason of the failure load reduction in false pullout failure. Additionally a lower shear resistance can also be observed at the part of perimeter towards the neighboring anchors for group anchor (see Figure 6). This reduction comes also from the tensile stresses existed in concrete between anchors due to the symmetric boundary condition and should be valid both for false pullout failure and pullout failure for group anchor. The increase of lateral tensile stresses in the concrete around the group anchors and the subsequent reduction of the shear resistant explains that, even in the case of pullout failure, the failure load of a quadruple anchor group may be smaller than 4 times the failure load of single anchor.

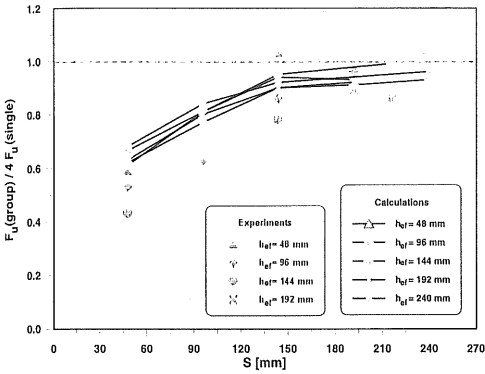


Fig. 7 Influence of anchor spacing on the failure of quadruple anchor group with bonded anchors ( $d = 12 \text{ mm}$ ,  $\tau_a \sim 12 \text{ N/mm}^2$ )

### 3.2 Group effect

For anchor groups with a spacing smaller than a critical value the failure load is reduced with decreasing spacing, which is called group effect. This can be seen from Figure 7, in which the calculated failure loads related to the failure load of a single anchor with the same embedment depth are plotted as a function of the spacing  $s$ . The Figure is valid for anchors with  $d = 12 \text{ mm}$ . If available experimental results by Lehr and Eligehausen (1998) are plotted as well. According to the results of Table 1 and Figure 7 it seems that two characteristic spacings exist to indicate the failure load of group anchors. We call these two characteristic spacings  $s_{cr1}$  and  $s_{cr2}$ , respectively. In the studied cases with  $d = 12 \text{ mm}$ ,  $s_{cr1}$  is equal to about  $150 \text{ mm}$  and  $s_{cr2}$  is about  $240 \text{ mm}$ . When the spacing is larger than  $s_{cr2}$ , there exists no group effect. For the spacings  $s_{cr1} \leq s \leq s_{cr2}$  the influence of the spacing on the failure load of a group with bonded anchors is relatively smaller and the

failure is caused by pullout failure. When the spacing is smaller than  $s_{cr1}$  the failure load is reduced significantly and the failure mode is mainly controlled by the failure of the concrete (CC failure, CCB failure or false pullout failure). In Figure 8 the described behavior is plotted schematically. However it seems to be sufficiently accurate to use the dotted straight line for the design of fastenings with bonded anchors. From Figure 7 and Table 1 it can be seen that the characteristic spacings  $s_{cr1}$  and  $s_{cr2}$  are not much influenced by the embedment depth. This means that the group effect is almost independent of the embedment depth in the investigated range ( $4 \leq h_{ef}/d \leq 20$ ).

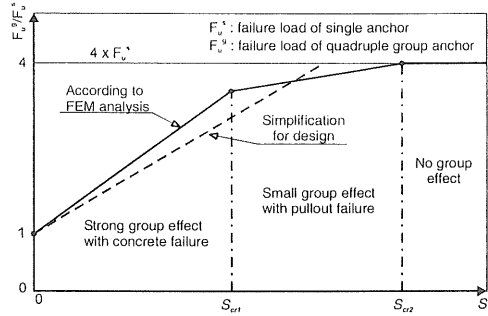


Fig. 8 Two characteristic spacing criterion and simplification for design

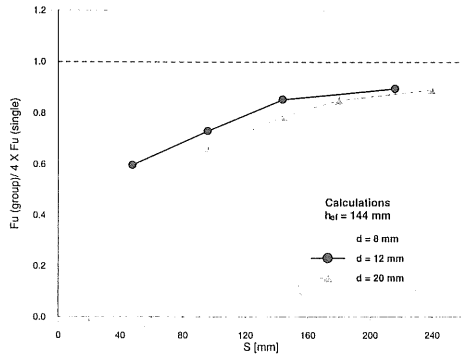


Fig. 9 Influence of anchor diameter on failure load of a quadruple anchor group with bonded anchors

### 3.3 Influence of anchor diameter on group effect

To study the influence of the anchor diameter on the group effect additional calculations with anchor diameters  $d = 8 \text{ mm}$  and  $d = 20 \text{ mm}$  were performed. The embedment depth was constant ( $h_{ef} = 144 \text{ mm}$ ). The calculated results are listed in Table 2 and plotted in Figure 9. For comparison, the calculated results for  $d = 12 \text{ mm}$  with the same embedment depth are presented as well. From this figure we can see that the characteristic spacings  $s_{cr1}$  and  $s_{cr2}$  are related

to the diameter  $d$ . This means that the characteristic spacings increase with increasing anchor diameter  $d$ . In the studied case the characteristic spacing  $s_{cr}$  is about 150 mm for anchor diameter  $d = 12$  mm. For the anchor diameter  $d = 8$  mm the spacing  $s_{cr}$  is reduced to about 100 mm and for  $d = 20$  mm it is increased to about 230 mm. However if we use the relative characteristic spacing  $s_{cr}/d$  we can see that the relative characteristic spacing  $s_{cr}/d$  is almost independent on the anchor diameter ( $s_{cr}/d = 12.5$  for  $d = 8$  mm;  $s_{cr}/d = 12.5$  for  $d = 12$  mm;  $s_{cr}/d = 11.5$  for  $d = 20$  mm).

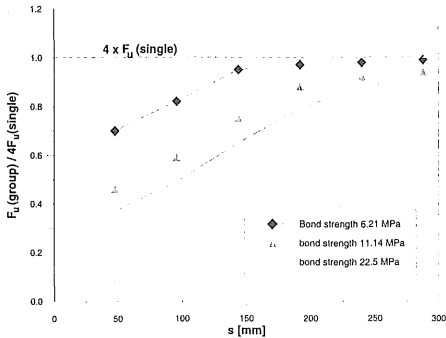


Fig. 10 Influence of bond strength on failure load of a quadruple group with bonded anchors ( $d = 16$  mm)

### 3.4 Influence of bond strength on the group effect

The bond strength plays a dominant role for the load transfer from the anchors to the concrete block. Therefore the group effect of bonded anchors should be influenced by the bond strength. In order to study this influence additional calculations with  $d = 16$  mm and  $h_{ef} = 96$  mm were performed. The bond strength was varied with  $\tau_u = 22.5$  N/mm<sup>2</sup> (high bond strength),  $\tau_u = 11.1$  N/mm<sup>2</sup> (average bond strength) and  $\tau_u = 6.2$  N/mm<sup>2</sup> (low bond strength), respectively. 7 cases were calculated with each bond strength, in which 6 cases are for anchor group and 1 case for a single anchor. The calculated failure loads and failure modes are listed in Table 3 and plotted in Figure 10. From this figure a significant influence of bond strength on the group effect can be observed. The characteristic spacing increases with the increase of bond strength. In the studied cases the characteristic spacings  $s_{cr}$  could be estimated as ~150 mm for a low bond strength ( $\tau_u = 6.2$  N/mm<sup>2</sup>), ~200 mm for a medium bond strength ( $\tau_u = 11.1$  N/mm<sup>2</sup>) and ~290 mm for a high bond strength ( $\tau_u = 22.5$  N/mm<sup>2</sup>). This means that with increasing bond strength the required spacing to ensure that the failure load of a quadruple fastenings is about 4 times the value for a single anchor increases with increasing bond strength. This is understandable be-

cause with increasing bond strength larger forces can be transmitted into the concrete by an anchor with a given diameter and embedment depth and therefore a larger concrete volume is needed to resist the forces.

## 4 CONCLUSIONS

- Four type of failure modes were observed in the calculations, which include concrete cone failure, pullout failure, combined concrete cone and bond failure and false pullout failure. The different failure mechanism and their influence on the group effect of bonded anchors have been revealed
- According to numerical and experimental results the failure load of quadruple bonded anchors in case of pullout failure may be smaller than 4 times the pullout failure load of single anchor. The reason of this lower failure load is mainly caused by the tensile strength in the concrete around anchors.
- Numerical and experimental results show that the failure load of quadruple anchor groups with bonded anchors increases with increasing anchor spacing. If the spacing is larger than a characteristic value  $s_{cr2}$  no group effect exists and the failure load at a quadruple group is 4 times the failure load of a single anchor. For  $s_{cr1} < s < s_{cr2}$ , a small group effect is exhibited with pullout failure. When  $s < s_{cr1}$ , a strong group effect occurs and the failure mode is mainly controlled by concrete failure.
- The characteristic spacings seems to be independent of the embedment depth in the investigated range ( $4 \leq h_{ef}/d \leq 20$ ).
- The absolute values of the characteristic spacings  $s_{cr1}$  and  $s_{cr2}$  are a function of the anchor diameter  $d$ . However the ratio of  $s_{cr1}/d$  and  $s_{cr2}/d$  are almost independent to the anchor diameter  $d$ .
- The group effect is influenced significantly by the bond strength. In the studied cases ( $d = 16$  mm,  $h_{ef} = 96$  mm) the characteristic spacing increases with increasing bond strength from  $s_{cr1} \sim 150$  mm ( $\sim 9d$ ,  $\tau_u = 6.2$  N/mm<sup>2</sup>) to  $s_{cr1} \sim 290$  mm ( $\sim 19d$ ,  $\tau_u = 22.5$  N/mm<sup>2</sup>).

## 5 REFERENCES

- Cook, R. A., Doerr, G.T. and Klingner, R.E. (1993) "Bond stress model for design of adhesive anchors." *ACI Structural Journal*, 90 (5): 514-524
- Cook, R. A., Kunz, J., Fuchs, W. and Konz, R. (1998) "Behavior and design of single adhesive anchors under tensile load in uncracked concrete." *ACI Structural Journal*, 95(1): 9-26

- Eligehausen, R., Mallee, R. and Rehm, G. (1984) "Befestigungen mit Verbundankern." *Betonwerk + Fertigteil-Technik*, Heft 10, 686-692; Heft 11, 781-785; Heft 12, 825-829
- Eligehausen, R., Mallee, R. and Rehm, G. (1997) "Befestigungstechnik (Fastening technique)." *Betonkalender 1997*, Ernst & Sohn, Berlin, pp 609-753
- Eligehausen, R., Lehr, B., Meszaros, J. and Fuchs, W. (1999) "Behavior and design of anchorage with bonded anchors under tension load." *Proc. of Int. Conference on Anchorage & Grouting towards the new Century*, 6-9 Oct. 1999, Guangzhou, China, Zhongshan University Publisher, pp 93-105
- Lehr, B. and Eligehausen, R. (1998) "Centric tensile tests of quadruple fastenings with bonded anchors." *Research report, Institut für Werkstoffe im Bauwesen*, Universität Stuttgart, not published
- Li, Y.-J., Ozbolt, J., Eligehausen, R. and Lehr, B. (1999) "3D numerical analysis of quadruple fastenings with bonded anchors." *CD-Rom Proc. of 13th ASCE Engineering Mechanics Division Conference*, 13-16 Jun. 1999, Baltimore, USA.
- Meszaros, J. and Eligehausen, R. (1998) "Auszieversuche mit Injektionsdübeln HIT-HY 150 bei gleichzeitiger Zweiachialbelastung des Ankergrundes" *Research report, Institut für Werkstoffe im Bauwesen*, Universität Stuttgart, not published
- Ozbolt, J., Li, Y.-J. and Kozar, I. (2000) "Microplane model for concrete with relaxed kinematic constraint" Accepted for publication in *Int. Journal of Solid and Structures*.
- Ozbolt, J. (1998) "MASA - Finite element program for nonlinear analysis of concrete and reinforced concrete structures." *Research report, Institut für Werkstoffe im Bauwesen*, Universität Stuttgart, not published.